Dark matter effects on the properties of neutron stars: Compactness and tidal deformability

Hong-Ming Liu (刘宏铭),[1,2] Jin-Biao Wei (魏金标),[3] and Zeng-Hua Li (李增花)[1,2,*]

[1]*Institute of Modern Physics, Key Laboratory of Nuclear Physics and Ion-Beam Application, MOE, Fudan University, Shanghai 200433, People's Republic of China*

[2]*Shanghai Research Center for Theoretical Nuclear Physics, NSFC and Fudan University, Shanghai 200438, China*

[3]*School of Mathematics and Physics, China University of Geosciences, Lumo Road 388, 430074 Wuhan, China*

G. F. Burgio, H. C. Das, and H.-J. Schulze

Istituto Nazionale di Fisica Nucleare, Sezione di Catania, Dipartimento di Fisica, Universitá di Catania, Via Santa Sofia 64, 95123 Catania, Italy

(Received 25 March 2024; accepted 24 May 2024; published 16 July 2024)

We systematically study the observable properties of dark-matter admixed neutron stars with arbitrary dark-matter fraction, employing a realistic nuclear equation of state in combination with self-interacting fermionic dark matter respecting constraints on the self-interaction cross section. Deviations from universal relations valid for nucleonic neutron stars are analyzed over the whole parameter space of the model and unequivocal signals for the presence of dark matter in neutron stars are identified.

DOI: 10.1103/PhysRevD.110.023024

I. INTRODUCTION

Dark matter (DM), realized by yet unknown elementary particles within or beyond the standard model [1–3], is one of the most enigmatic aspects of current astrophysics [4,5]. It must make up nearly 90% of the matter in the Universe in order to explain observations at Galactic and super-galactic scales [6–10]. Most of its properties like its mass and interactions with other particles are presently unknown [11–14].

Theoretically, several kinds of bosonic and fermionic DM candidates have been hypothesized, such as a weakly-interacting massive particle [15–19], especially neutralino [20–28], asymmetric dark matter [29–32] like mirror matter [33–35], axion [36,37], and strangelets [38–41].

A particular environment to reveal features of DM are neutron stars (NSs), the densest objects known in the Universe, for which more and more precise observational data become available. Their hypothetical capability to accumulate DM might provide possibilities to deduce related DM properties. It is thus of great interest to theoretically analyze DM-admixed NS (DNS) models, combining a more or less well-known nuclear-matter equation of state (NM EOS) with a hypothetical DM EOS within a general-relativistic two-fluid approach [34,42,43].

The fundamental theoretical challenge of the eventual presence of DM in NSs is the fact that their mass-radius relation is not anymore a unique function, but depends on an additional degree of freedom, the DM content. The absence of any knowledge regarding the nature of DM, combined with the persisting uncertainty of the high-density NM EOS, then renders any theoretical conclusion regarding either DM or high-density NM doubtful. The simplest example would be the observation of a very massive "NS," which could simply be caused by the presence of a massive DM halo, but also by a very stiff NM EOS. Therefore, theoretical methods have to be devised to unequivocally identify the presence and quantity of DM in NSs.

It is generally believed that most or all observed NSs are such, namely standard hadronic stars with very little admixture of DM. We note at this point that current estimates of the acquired DM content by accretion during the NS lifetime yield extremely small results of $\lesssim 10^{-10} M_\odot$ [13,15,17,29,30,32,44–47], which would be unobservable. The existence of DNSs with large DM fractions (of the order of percent or larger) assumed in this article, therefore requires exotic capture or formation mechanisms [12,47–54], which remain so far very speculative. Keeping this in mind, we study in this work in a qualitative manner DNSs with arbitrary DM fraction up to 100%, corresponding to pure dark stars (DSs) [50,55–57].

The effects of DM on the properties of NM and NSs have been intensely investigated in recent years. Apart from its

*zhli09@fudan.edu.cn

fundamental impact on NS mass and radius [11,58–64], a large number of works studied the possibility of DM acquisition by NSs [65–70] and related phenomena like heating [14,17,44,46,71–75] or internal black hole formation and collapse [15,18,30,32,34,45,76–79]. Recently, more quantitative studies have been performed, like the DM effects on the derived properties of NM [23], or the validity of universal relations between the NS compactness M/R and the moment of inertia I, tidal deformability Λ, and quadrupole moment Q [80–83], in the presence of DM [51,84,85]. References [86,87] examined the possibility of the LIGO/Virgo events GW170817 [88] and GW190425 [89] being realized by a DNS scenario and Ref. [24] for the GW190814 [90] event. Many recent works [22,24–26,28,35,51–53,91–99] focused on DM effects on the NS tidal deformability and related observables [100–103], which are directly accessible by recent and future gravitational wave (GW) detectors. The impact of DM on the pulsar x-ray profile [104,105] and on NS cooling processes [19,27] were also examined recently.

The purpose of the present article is to continue and extend our previous study of DNS optical radii and tidal deformability [106] over the full parameter space of a given DM model. We will now assume self-interacting fermionic DM particles with an interaction strength constrained by observational limits on the self-interaction cross section.

The optical radius R_N is perhaps the most relevant and, at the same time, the most easily accessible observable of a NS (apart from the gravitational mass M) and therefore merits particular attention before studying more intricate features of a NS. We will also analyze the validity and breakdown of universal relations between stellar compactness M/R_N and tidal deformability Λ. The purpose is to devise unequivocal methods to deduce and quantify the presence of DM in NSs.

This article is organized as follows. In Sec. II, the EOSs of ordinary NM and DM used in this work are briefly described. The detailed calculations and discussion are presented in Sec. III. A summary is given in Sec. IV.

II. FORMALISM

A. Equation of state for nuclear matter

As in [106], we employ here the latest version of a Brueckner-Hartree-Fock EOS obtained with the Argonne V18 NN potential and compatible three-body forces [107–109], see [110,111] for a more detailed account. This EOS is compatible with all current low-density constraints [112–114] and, in particular, also with those imposed on NS maximum mass $M_{\rm max} > 2M_\odot$ [115–117], radius $R_{1.4} \approx 11$–13 km [118–121], and tidal deformability $\Lambda_{1.4} \approx 70$–580 [88,122–124].

Therefore, observation of compact objects violating these constraints (e.g., a $\Lambda_{1.4}$ outside the range [70,580]) might be interpreted as indicating DM admixture according to the following detailed analysis.

B. Equation of state for dark matter

We employ in this work the frequently used [49,51–53,59,61,92,93,96,125–127] DM model of fermions with mass μ self-interacting via a repulsive Yukawa potential,

$$V(r) = \alpha \frac{e^{-mr}}{r}, \tag{1}$$

with coupling constant α and mediator mass m. Following Ref. [125] we write pressure and energy density of the resulting DM EOS as

$$p_D = \frac{\mu^4}{8\pi^2}[x\sqrt{1+x^2}(2x^2/3-1) + \mathrm{arsinh}(x)] + \delta, \tag{2}$$

$$\epsilon_D = \frac{\mu^4}{8\pi^2}[x\sqrt{1+x^2}(2x^2+1) - \mathrm{arsinh}(x)] + \delta, \tag{3}$$

where

$$x = \frac{k_F}{\mu} = \frac{(3\pi^2 n)^{1/3}}{\mu} \tag{4}$$

is the dimensionless kinetic parameter with the DM particle density n, and the self-interaction term is written as

$$\delta = \frac{2}{9\pi^3}\frac{\alpha\mu^6}{m^2}x^6 \equiv \mu^4\left(\frac{y}{3\pi^2}\right)^2 x^6 = \left(\frac{yn}{\mu}\right)^2, \tag{5}$$

introducing the interaction parameter $y^2 = 2\pi\alpha\mu^2/m^2$. Reference [125] contains interesting scaling relations regarding the EOS and mass-radius relations of pure fermionic DM stars.

Within this model, y is not a free parameter, but constrained by observational limits imposed on the DM self-interaction cross section σ [128–131],

$$\sigma/\mu \sim 0.1 - 10\ \mathrm{cm}^2/\mathrm{g}. \tag{6}$$

In [49,51,126] it has been shown that the Born approximation,

$$\sigma_{\rm Born} = \frac{4\pi\alpha^2}{m^4}\mu^2 = \frac{y^4}{\pi\mu^2}, \tag{7}$$

is very accurate for $\mu \lesssim 1$ GeV and in any case remains valid in the limit $\alpha \to 0$ for larger masses. We therefore employ here this approximation, choosing for simplicity the fixed constraint

$$\sigma/\mu = 1\ \mathrm{cm}^2/\mathrm{g} = 4560/\mathrm{GeV}^3, \tag{8}$$

which appears compatible with all current observations. This implies

$$y^4 = \pi\mu^3\sigma/\mu \sim \pi(16.58\mu_1)^3, \tag{9}$$

$$y \sim 10.94\mu_1^{3/4} \tag{10}$$

with $\mu_1 \equiv \mu/1$ GeV. After this, the DM EOS depends only on the parameter μ.

This is demonstrated in Fig. 1, which compares the DM EOS with and without self-interaction for four typical masses $\mu = 0.5, 1, 2, 4$ GeV, in comparison with the nucleonic EOS. Markers indicate the configurations of maximum stellar mass. It can be seen that the self-interaction is always important in the relevant density domains and stiffens substantially the EOS. The nucleonic EOS exhibits different trends for core, inner crust, and outer crust of a NS.

C. Hydrostatic configuration

The stable configurations of the DNSs are obtained from a two-fluid version of the Tolman-Oppenheimer-Volkoff equations [34,42,43]:

$$\frac{dp_D}{dr} = -[p_D + \epsilon_D]\frac{d\nu}{dr}, \tag{11}$$

$$\frac{dp_N}{dr} = -[p_N + \epsilon_N]\frac{d\nu}{dr}, \tag{12}$$

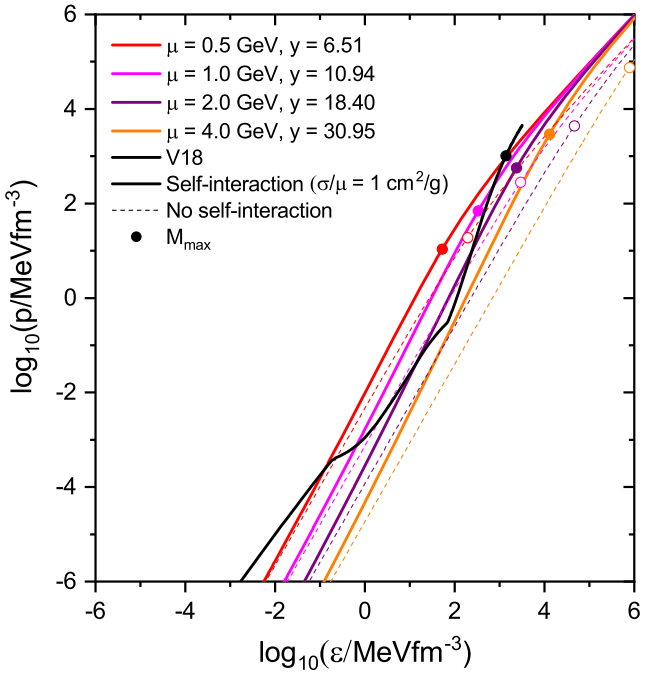

FIG. 1. EOSs of different pure DM models and the nuclear V18 EOS. The markers indicate the values of the maximum-mass $M_{\max}$ configurations. The interaction parameter y, Eq. (10), is also listed.

$$\frac{dm}{dr} = 4\pi r^2\epsilon, \tag{13}$$

$$\frac{dN_i}{dr} = \frac{4\pi r^2 n_i}{\sqrt{1-2m/r}}, \tag{14}$$

$$\frac{d\nu}{dr} = \frac{m + 4\pi r^3 p}{r(r-2m)}, \tag{15}$$

where r is the radial coordinate from the center of the star, and $p = p_N + p_D$, $\epsilon = \epsilon_N + \epsilon_D$, $m = m_N + m_D$ are the total pressure, energy density, and enclosed mass, respectively. In addition, N_i are the enclosed particle numbers with the corresponding densities $n = k_F^3/3\pi^2$.

The total gravitational mass of the DNS is

$$M = m_N(R_N) + m_D(R_D), \tag{16}$$

where the stellar radii R_N and R_D are defined by the vanishing of the respective pressures. There are thus, in general, two scenarios: DM-core ($R_D < R_N$) or DM-halo ($R_D > R_N$) stars.

It has been shown in stability analyses of the two-fluid model [64,93,132–136] that the limits of stellar stability occur at the maximum of M along fixed-particle-number contours, which have been demonstrated [93,133] to coincide with the maximum of the $M(R)$ relations for fixed DM fraction f, just as in the limit of ordinary NSs. Configurations with larger central density (smaller radius) are unstable with respect to induced radial oscillations, as verified in the above references. We show and discuss only stable DNS configurations in the following.

We first analyze the mass-radius relations of pure DSs in Fig. 2, comparing the results with and without self-interaction for various values of μ. Consistent with the DM EOS, one notes that the self-interaction is always very important and leads to stars with much larger masses and radii for the same μ. In this work we only employ values of $\mu \sim \mathcal{O}(1\text{ GeV})$, such that the corresponding values of $M_{\max}$ are of the same order as those of ordinary NSs, $\sim\mathcal{O}(1M_\odot)$, for which the mass-radius relation of the nucleonic V18 EOS is shown for comparison. Otherwise, the observable effects on NS structure will be very small [106]. We note that in [125] the following scaling relations for $M_{\max}$ and the corresponding radius $R(M_{\max})$ were derived for $y \gg 1$,

$$M_{\max}/M_\odot = (0.627 + 0.269y)/\mu_1^2 \tag{17}$$

$$= (0.627 + 2.943\mu_1^{3/4})/\mu_1^2, \tag{18}$$

$$R(M_{\max})/\text{km} = (8.114 + 1.921y)/\mu_1^2, \tag{19}$$

$$= (8.114 + 21.01\mu_1^{3/4})/\mu_1^2, \tag{20}$$

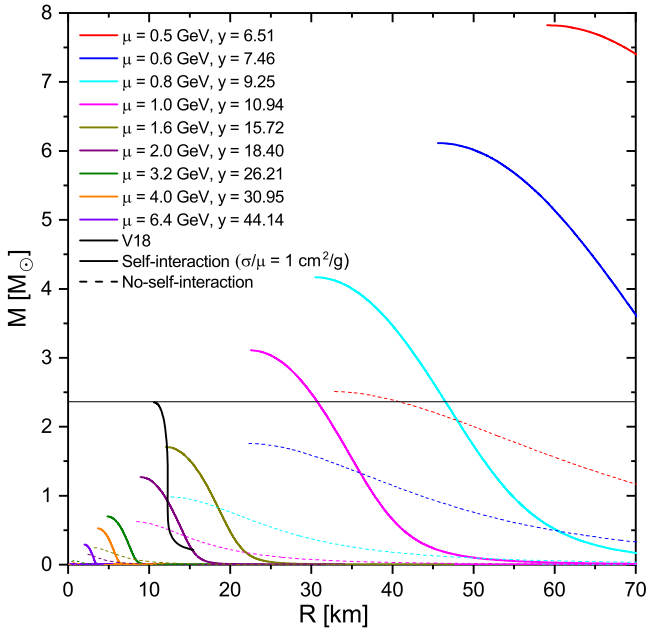

FIG. 2. Mass-radius relations of pure dark stars for different values of the DM particle mass μ, with (solid) and without (dashed) self-interaction, in comparison with the NM EOS V18 (solid black). The horizontal black line indicates the maximum mass of a pure NS, $M_{\max} = 2.36M_\odot$.

which are reasonably well fulfilled for our range of μ and associated y, Eq. (10), given also in the figure.

After analyzing our models of pure NSs and pure DM stars, we now examine, in detail, the properties of DNSs within the two-fluid scenario, assuming that the two fluids interact only via gravity. The resulting scenario is very rich because the stellar configurations depend on the DM fraction $f = M_D/M$. The following Fig. 3 gives a detailed account of the possible mass-radius relations of DNSs (including DM self-interaction) with $\mu = 1$ GeV over the full range of DM fraction f. Both $M(R_N)$ and $M(R_D)$ relations, Eq. (16), are shown as solid or dotted curves, respectively.

The maximum gravitational mass is $2.36M_\odot$ for the $f = 0$ pure NS (black solid curve) and $3.11M_\odot$ for the $f = 1$ pure DS in this case (orange dotted curve), whereas intermediate mixed stars have lower $M_{\max}$. Those are plotted in intervals of f varying by 0.02. One can classify the stars as either DM core or DM halo, and for each fixed-f curve a marker denotes the transition $R_D = R_N$ between these configurations, if present. For example, for $f = 0.1$ all stars are DM core, whereas for $f = 0.2$ there are two transitions at $(M, R) = (1.69M_\odot, 10.64\ \text{km})$ and $(M, R) = (0.18M_\odot, 15.69\ \text{km})$ from DM core to DM halo and back. Many (M, R_N) points are double or triple occupied, as, for example, the $f = 0.1$, 0.9, 0.99994 stars with a common $(M, R_N) = (1.11M_\odot, 11.07\ \text{km})$. These multiple-occupied

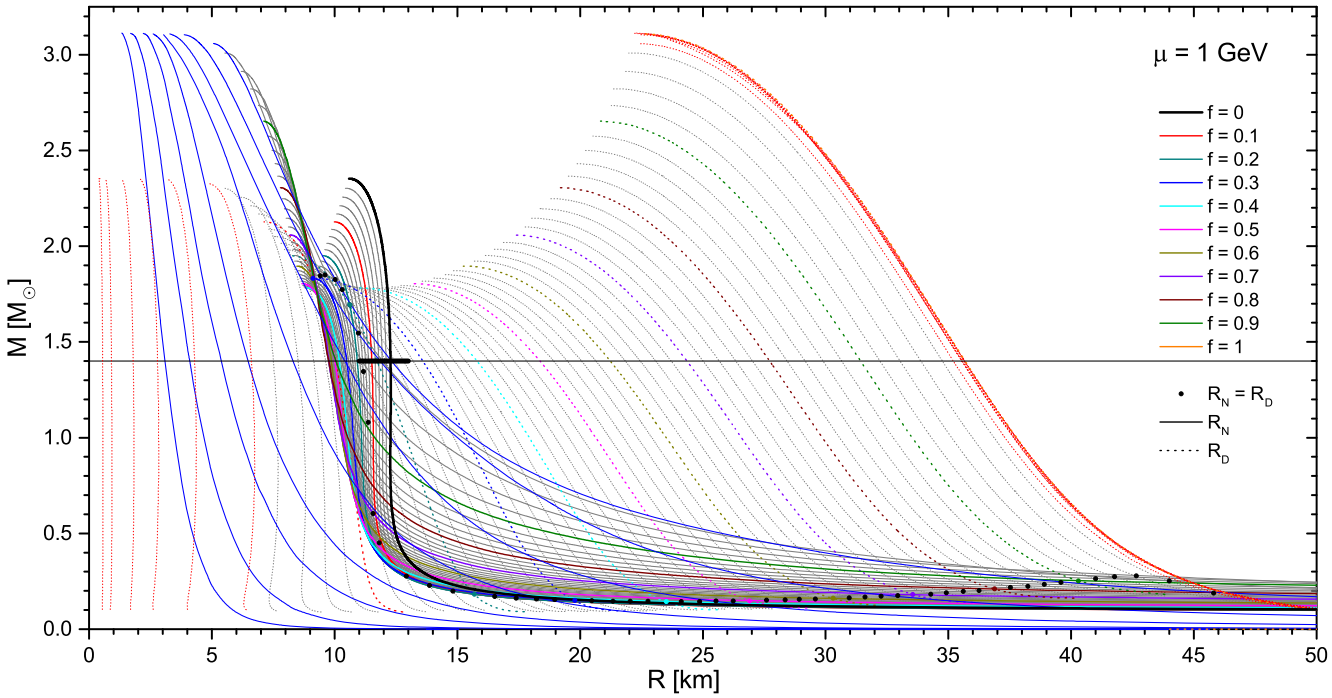

FIG. 3. Total gravitational mass M as a function of nuclear (solid curves) or dark (dotted curves) radius for the $\mu = 1$ GeV model with different DM fractions $f = M_D/M$. Markers indicate $R_D = R_N$ configurations. The range of NS radii $R_{1.4} = 11$–13 km is represented by a horizontal bar on the $M = 1.4M_\odot$ line. The values of f are in intervals of 0.02, apart from those close to the boundaries: $f = 10^{-2,-3,\ldots,-7}$ (thin dotted red curves) and $f = 1 - 10^{-2,-3,\ldots,-9}$ (thin solid blue curves).

configurations, characterized by different f, belong to the class of the so-called "twin" stars, which differ substantially in their internal structure and DM radius, but would be indistinguishable by just mass and optical radius observations. A more detailed discussion can be found in [106].

Another interesting aspect are configurations of nearly pure NSs or DSs, with a very small fraction of the minority component. Those correspond to small amounts of minority matter trapped in a container majority star and are characterized by small minority radii. Those are shown in the figure by thin solid blue curves ($f \to 1$) for DSs containing a small amount of pure NM, plotted in intervals of $f = 1 - 10^{-2,-3,\ldots,-9}$, or thin dotted red ($f \to 0$) curves which correspond to pure NM configurations with a tiny amount of DM equal to $f = 10^{-2,-3,\ldots,-7}$.

According to this discussion, one can prepare for a given μ, a configuration plot in the (M, R_N) plane [64,106], that shows all possible DM-core or DM-halo stars, corresponding to the domain covered by solid curves in Fig. 3, for example. This is done in Fig. 4 for $\mu = 0.8, 1.6, 3.2, 6.4$ GeV. According to the previous discussion, magenta domains contain only DM-core stars, delimited by the black solid curve ($f = 0$), whereas the green domains (dark green $f < 0.99$ and light green $f > 0.99$ for clarity) host only DM-halo stars. In the cyan domain both kinds of configurations are present. One notes that for "large" μ nearly all stellar configurations are DM core (magenta), and added DM causes always a reduction of radius and maximum DNS mass. However, these possible changes become smaller and smaller with increasing μ. With decreasing μ instead, DM-halo configurations (green) become increasingly dominant. They feature a wide range of possible optical radii R_N from zero (for very diluted NM, $f \to 1$) to very large values $\gg R(f = 0)$. Also the possible maximum mass becomes larger than the pure NS one for $\mu < 1.11$ GeV, increasing with decreasing μ.

Therefore, the possible DNS configurations depend strongly on the DM particle mass μ, and this fact can be exploited to conversely deduce the values of μ and f from eventual DNS observations. This possibility will be examined in detail in the following.

III. RESULTS

A. Mass and radius

We begin in Fig. 5 with the most significant observables, mass and radius, namely the maximum mass $M_{\max}$ (a) and the optical radii $R_{1.4}^{(N)}$ (b) and $R_{2.0}^{(N)}$ (c) as contour plots of the two model parameters μ and f. According to the preceding discussion, and roughly dividing into the cases $\mu \gtrsim 1$ GeV and $\mu \lesssim 1$ GeV, in the first case $M_{\max} < M_{\max}(f = 0) = 2.36 M_\odot$ (indicated by a red contour) for any f (mostly DM-core stars), whereas in the second case $M_{\max}$ might reach very large values with increasing f (all DM-halo stars). As an illustrative example, we evidence the (yellow) $2.6 M_\odot$ contour, corresponding to the lighter object in GW190814 [90], being either a black hole or an "exotic" NS, in this case a DM-halo DNS [24]. This is, of course, possible in the present framework for sufficiently small values of μ and large values of f, and the $2.6 M_\odot$ contour indicates the suitable (f, μ) values in the plot, in the absence of any other information regarding this object. The (red) $M = 1.4 M_\odot$ contour identifies the maximum value of μ as a function of f, for which a stable $1.4 M_\odot$ DNS is possible.

We examine the optical radius $R_{1.4}^{(N)}$ of such stars in panel (b). Again dividing roughly into the two cases, for high masses $\mu \gtrsim 1$ GeV there are only DM-core stars, where the

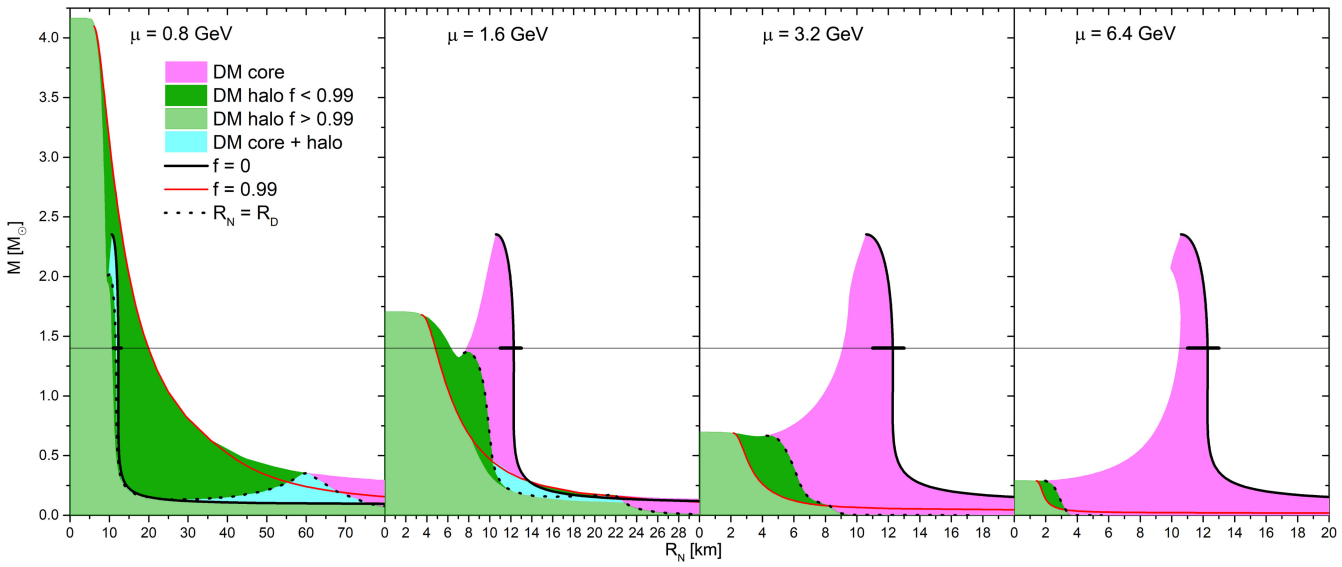

FIG. 4. The domains of stable DM-core (magenta shading), DM-halo (green), and both (cyan) DNSs in the (M, R_N) plane for different DM models. Note the different R_N axes. See extended discussion in the text.

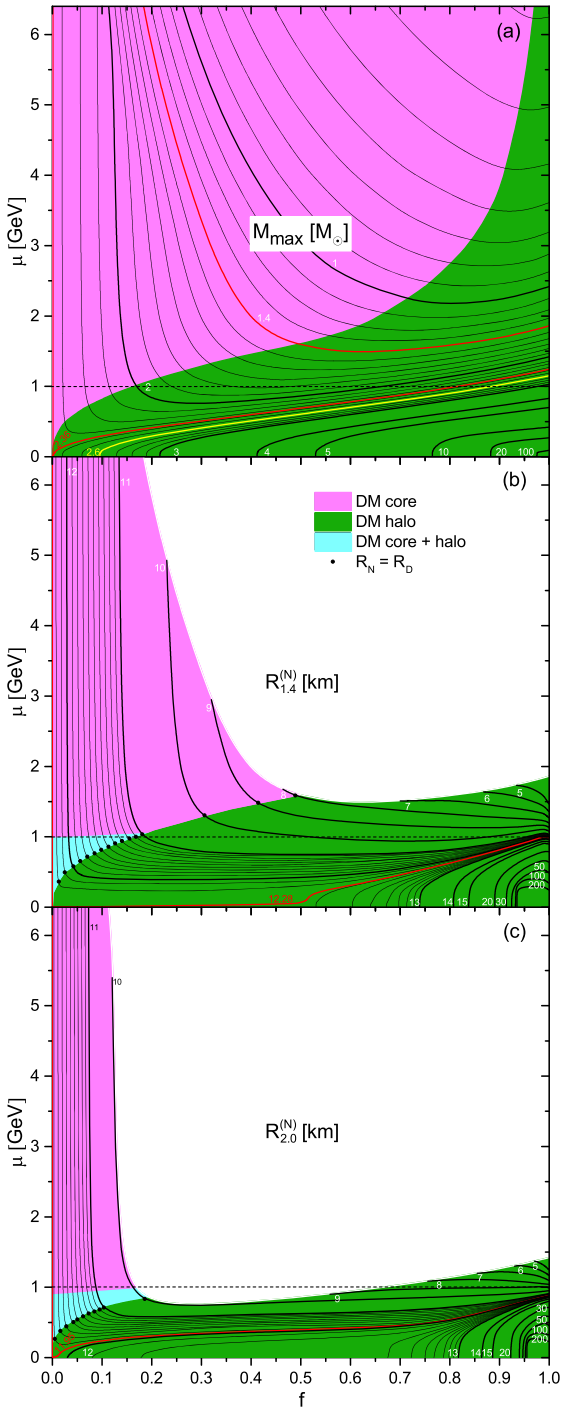

FIG. 5. Contour plots of (a) $M_{\max}$ [thin contours are in intervals of $0.1M_\odot$; 2.36 (red) is the value for the pure NS; 2.6 (yellow) is the value for the heavy object in GW190814] and (b) and (c) optical $R_{1.4}^{(N)}$ and $R_{2.0}^{(N)}$ [indicated by numbers in km; thin contours are in intervals of 0.1 km; 12.28 and 11.95 are the values for the pure NS], as functions of (f,μ). The color scheme is as in Fig. 4. The horizontal dashed line at $\mu = 1$ GeV is to guide the eye.

DM core pulls together also the nuclear matter, always reducing the radius with increasing f from the $f = 0$ pure NS value 12.28 km. The maximum possible DM fraction f is limited in this regime by the condition that a stable $1.4M_\odot$ DNS can be formed, see panel (a).

On the other hand, most $\mu \lesssim 1$ GeV configurations are DM halo, without upper limits on f, and for sufficiently large f also the optical radius is stretched out to large values by the surrounding DM halo. This concurs with very large $M_{\max}$ in panel (a). These stars feature "low-density" NM (described by the NS crust EOS in this work) embedded in a larger DM "container" star. Similar as pointed out for Fig. 3, in this domain for a fixed μ two or three configurations with the same $R_{1.4}^{(N)}$ but different f (and different $R_{1.4}$) exist; therefore, only knowing μ and $R_{1.4}^{(N)}$, a unique classification of a DNS is not possible here.

Qualitatively similar results for $R_{2.0}^{(N)}$ are shown in panel (c). Naturally the parameter space is more restricted here due to the $M = 2M_\odot$ condition, see panel (a).

B. Tidal deformability

An observable closely related to the radius R is the tidal deformability (quadrupole polarizability) Λ, obtained from the tidal Love number k_2 [137–141],

$$\Lambda = \frac{2}{3}\left(\frac{R}{M}\right)^5 k_2, \tag{21}$$

where R is the gravitational-mass radius, i.e., the outer DNS radius in our formalism. The relevant equations to compute k_2 in the two-fluid formalism can be found in [93–95,103], for example.

In Fig. 6(a) we display $(k_2)_{1.4}(f,\mu)$ as a contour plot, just as $R_{1.4}^{(N)}$ in Fig. 5(b). One can see that for not very large values of f the effect of DM admixture is always a reduction of k_2. Only for very dark stars with $f \gtrsim 0.8$ values of $k_2 > 0.086$ (the one of a pure NS) are reached again. However, k_2 is not directly observable, but the relevant quantity is the tidal deformability $\Lambda_{1.4}(f,\mu)$ shown in panel (b). Obviously, the dependence of $\Lambda_{1.4}$ on the fifth power of the radius $R_{1.4}$ then implies also a very strong dependence on (f,μ) that can clearly be seen in the figure. For DM-core configurations $\Lambda_{1.4}$ is reduced compared to the pure NS value 430 (red contour), as is the radius $R_{1.4} = R_{1.4}^{(N)}$ reported in Fig. 5(b), whereas for DM-halo configurations with large f and $R_{1.4} = R_{1.4}^{(D)}$, $\Lambda_{1.4}$ becomes enormous. Thus any nontiny admixture of DM causes a substantial effect that we analyze as follows.

A universal relation between the tidal deformability and the compactness M/R of pure NSs was introduced in

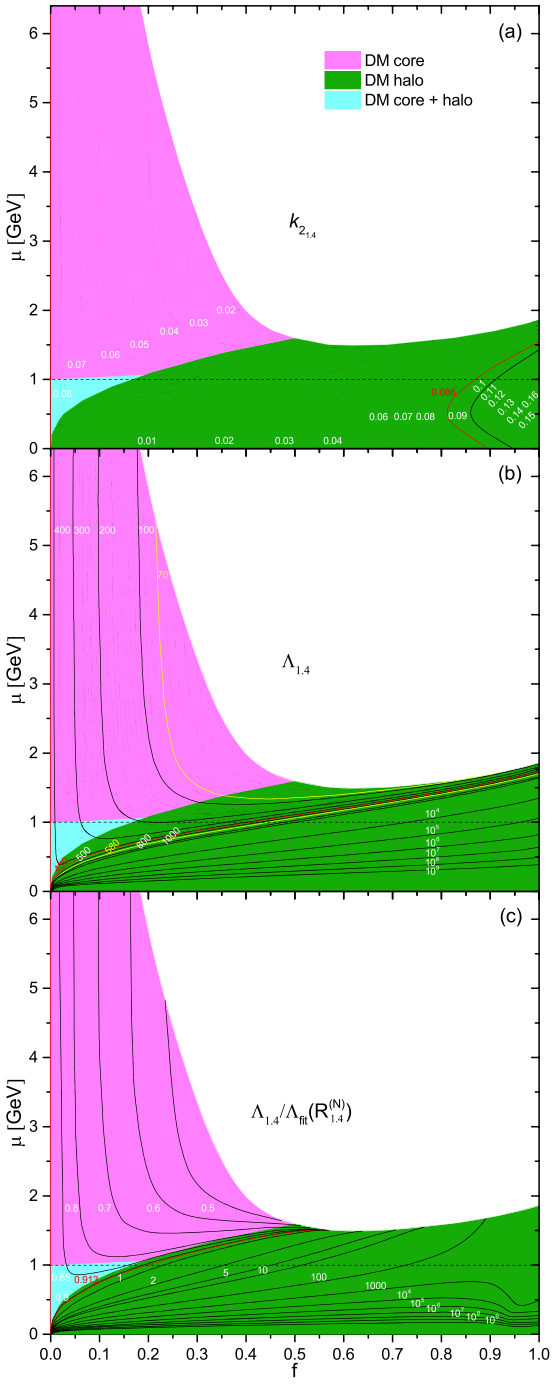

FIG. 6. Contour plots of (a) Love number $(k_2)_{1.4}$ (contours are in intervals of 0.01; 0.086 is the value for the pure NS), (b) tidal deformability $\Lambda_{1.4}$ (thin contours are in intervals of 10; 430 is the value for the pure NS), and (c) the ratio $\Lambda_{1.4}/\Lambda_{\rm fit}(R^{(N)}_{1.4})$, Eq. (23), as functions of (f,μ). The color scheme is as in Fig. 4. The horizontal dotted line at $\mu = 1$ GeV is to guide the eye. The range $\Lambda_{1.4} = 70$–580 attributed to GW170817 [122] is limited by yellow contour lines.

Ref. [80], and in Refs. [82,124] the following fit was proposed:

$$\frac{M}{R} = 0.36 - 0.0355\ln\Lambda + 0.000705(\ln\Lambda)^2, \quad (22)$$

or equivalently

$$\log\Lambda_{\rm fit}(R) = 10.9 - 16.4\sqrt{\frac{M}{R} + 0.087}, \quad (23)$$

which holds to within 7% for a large set of NS nucleonic EOSs [82]. Recently an equivalent but more sophisticated fit was derived in [83]. Substantial deviations from this fit formula therefore indicate "non-nucleonic" compact stars, and we illustrate this by displaying in Fig. 6(c) the ratio $\Lambda_{1.4}/\Lambda_{\rm fit}(R^{(N)}_{1.4})$ between the DNS value and the expected value of a pure NS with the same optical radius $R^{(N)}_{1.4}$ as the DNS.

In the $\mu \gtrsim 1$ GeV DM-core regime we have $R^{(N)}_{1.4} = R_{1.4}$, and therefore, the reduction of $\Lambda_{1.4}$ simply reflects the moderate reduction of the radius in this domain, leading also to a moderate reduction of $\Lambda_{1.4}/\Lambda_{\rm fit}(R^{(N)}_{1.4})$. However, in the $\mu \lesssim 1$ GeV DM-halo regime with $R^{(N)}_{1.4} \ll R_{1.4}$, apart from the very large values of $\Lambda_{1.4}$ due to the extended halo, the value of $\Lambda_{\rm fit}(R^{(N)}_{1.4})$ is also too small and this amplifies the ratio $\Lambda_{1.4}/\Lambda_{\rm fit}(R^{(N)}_{1.4})$ even more, to increases of several orders of magnitude with $f \to 1$ but, in particular, $\mu \to 0$. Thus DNSs in this regime should exhibit very clear observational signatures by just analyzing their optical radius and tidal deformability, in the way just presented.

To be specific, suppose a future GW event (or other type of observation) allows to determine independently both $\Lambda_{1.4}$ and $R^{(N)}_{1.4}$ of an object. Then a substantial difference between $\Lambda_{1.4}$ and $\Lambda_{\rm fit}(R^{(N)}_{1.4})$ would indicate an unequivocal signal for DM, since for all nucleonic stars $\Lambda \approx \Lambda_{\rm fit}$, as given by the universal relation. For example, an observational value $\Lambda_{1.4}/\Lambda_{\rm fit}(R^{(N)}_{1.4}) = 10$ would mean that the observation could only be described by a DNS with (f,μ) values lying on the ten contour in Fig. 6(c), and the value of $\Lambda_{1.4}$ or $R^{(N)}_{1.4}$ then allows to determine μ and f separately.

For a different illustration of this feature, we compare in Fig. 7 explicitly the universal relation $\Lambda_{\rm fit}(M/R_N)$ (wide curve) with the actual DNS relations (dashed curves) for either fixed $\mu = 1$ GeV (a) or fixed $f = 0.1$ (b), varying the other variable. The enormous enhancement of Λ relative to $\Lambda_{\rm fit}$ for DM-halo stars is evident in both cases, increasing with $f \to 1$ and $\mu \to 0$, respectively, as explained before. The results for the $M = 1.4M_\odot$ configurations (square markers) in the figure correspond to those analyzed

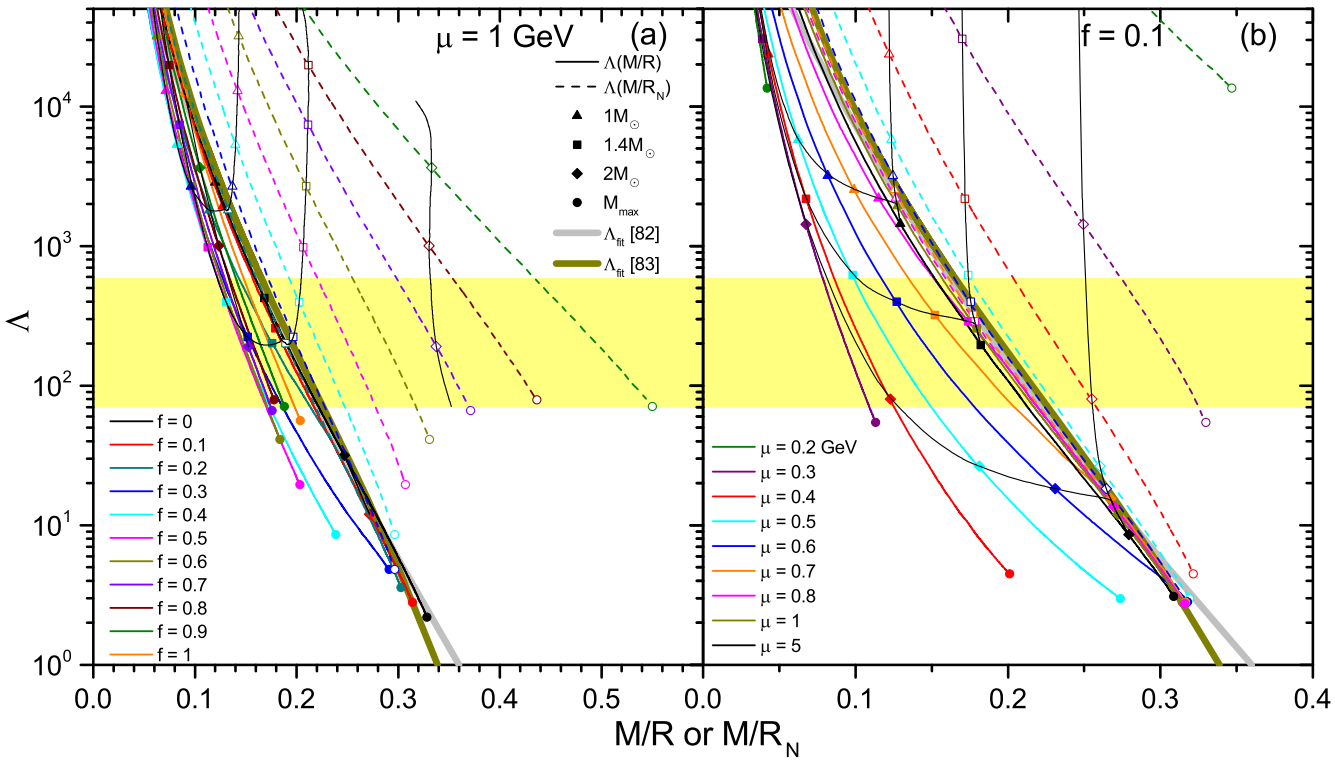

FIG. 7. Λ vs M/R (solid curves) and M/R_N (dashed curves) for (a) $\mu = 1$ GeV, varying f and (b) $f = 0.1$, varying μ. Configurations of fixed $M = 1, 1.4, 2M_\odot, M_{\max}$ are indicated by markers and joined by black lines. The universal relations for pure NSs of [82,83] are shown as wide curves. The shaded band indicates the range 70–580 for $M = 1.4M_\odot$ (square markers) deduced from GW170817 [122].

before in Figs. 5 and 6, but the qualitative behavior is the same for any mass M (or compactness M/R). Equivalent results but limited to very small DM fractions were also obtained recently in [84,85]. Thus simultaneous measurement of M, R_N, and Λ can unequivocally determine whether the star contains DM (off the $\Lambda_{\rm fit}$ curve) or not (on the $\Lambda_{\rm fit}$ curve).

Regarding the particular case of GW170817, it is obvious that the only constraint $\Lambda_{1.4} = 70$–580 is compatible with a very wide range of parameters (f, μ), as can be seen more clearly in Fig. 6(b). This is due to the large uncertainty of $\Lambda_{1.4}$; a precise measured value of $\Lambda_{1.4}$ together with the value of $R_{1.4}^{(N)}$ would also determine (f, μ) precisely (supposedly to $f = 0$, a pure NS).

The figure, in addition, shows the relation between Λ and the true compactness M/R (solid curves), should one be able to deduce the gravitational radius R observationally. In this case the actual values lie always below the fit formula due to the large difference between R and R_N in DM-halo stars. Thus also in this kind of analysis there would be a unique signature of DM in DNSs.

IV. SUMMARY

We have analyzed the properties of stable DNSs with substantial DM fraction, combining a well-constrained nucleonic EOS with a fermionic DM EOS respecting an important constraint on the self-interaction cross section. The analysis was focused on the most important and accessible observables: mass, radius, and tidal deformability. Already, at this level, there are very pronounced observational features (violation of universal relations) that would clearly discern a DNS from a "standard" NS, provided the DM fraction is not tiny. Registration of future GW events will allow to perform such analysis with good precision, allowing a search for DM in this way.

ACKNOWLEDGMENTS

This work is sponsored by the National Key R&D Program of China No. 2022YFA1602303 and the National Natural Science Foundation of China under Grants No. 11975077, No. 12147101, and No. 12205260.

[1] F. Zwicky, Gen. Relativ. Gravit. **41**, 207 (2009).
[2] G. Bertone, D. Hooper, and J. Silk, Phys. Rep. **405**, 279 (2005).
[3] J. L. Feng, Annu. Rev. Astron. Astrophys. **48**, 495 (2010).
[4] V. Trimble, Annu. Rev. Astron. Astrophys. **25**, 425 (1987).
[5] L. Bergström, Rep. Prog. Phys. **63**, 793 (2000).
[6] K. G. Begeman, A. H. Broeils, and R. H. Sanders, Mon. Not. R. Astron. Soc. **249**, 523 (1991).
[7] E. Abdalla, L. R. Abramo, L. Sodré, and B. Wang, Phys. Lett. B **673**, 107 (2009).
[8] E. Abdalla, L. R. Abramo, and J. C. C. de Souza, Phys. Rev. D **82**, 023508 (2010).
[9] D. M. Wittman, J. A. Tyson, D. Kirkman, I. Dell'Antonio, and G. Bernstein, Nature (London) **405**, 143 (2000).
[10] R. Massey, T. Kitching, and J. Richard, Rep. Prog. Phys. **73**, 086901 (2010).
[11] A. B. Henriques, A. R. Liddle, and R. G. Moorhouse, Nucl. Phys. **B337**, 737 (1990).
[12] P. Ciarcelluti and F. Sandin, Phys. Lett. B **695**, 19 (2011).
[13] T. Güver, A. E. Erkoca, M. H. Reno, and I. Sarcevic, J. Cosmol. Astropart. Phys. 05 (**2014**) 013.
[14] N. Raj, P. Tanedo, and H.-B. Yu, Phys. Rev. D **97**, 043006 (2018).
[15] I. Goldman and S. Nussinov, Phys. Rev. D **40**, 3221 (1989).
[16] S. Andreas, T. Hambye, and M. H. G. Tytgat, J. Cosmol. Astropart. Phys. 10 (2008) 034.
[17] C. Kouvaris, Phys. Rev. D **77**, 023006 (2008).
[18] C. Kouvaris, Phys. Rev. Lett. **108**, 191301 (2012).
[19] S. A. Bhat and A. Paul, Eur. Phys. J. C **80**, 544 (2020).
[20] D. Hooper and L.-T. Wang, Phys. Rev. D **69**, 035001 (2004).
[21] G. Panotopoulos and I. Lopes, Phys. Rev. D **96**, 083004 (2017).
[22] A. Das, T. Malik, and A. C. Nayak, Phys. Rev. D **99**, 043016 (2019).
[23] H. C. Das, A. Kumar, B. Kumar, S. K. Biswal, T. Nakatsukasa, A. Li, and S. K. Patra, Mon. Not. R. Astron. Soc. **495**, 4893 (2020).
[24] H. C. Das, A. Kumar, and S. K. Patra, Phys. Rev. D **104**, 063028 (2021).
[25] H. C. Das, A. Kumar, and S. K. Patra, Mon. Not. R. Astron. Soc. **507**, 4053 (2021).
[26] H. C. Das, A. Kumar, B. Kumar, and S. K. Patra, Galaxies **10**, 14 (2022).
[27] A. Kumar, H. C. Das, and S. K. Patra, Mon. Not. R. Astron. Soc. **513**, 1820 (2022).
[28] O. Lourenço, C. H. Lenzi, T. Frederico, and M. Dutra, Phys. Rev. D **106**, 043010 (2022).
[29] C. Kouvaris and P. Tinyakov, Phys. Rev. D **83**, 083512 (2011).
[30] S. D. McDermott, H.-B. Yu, and K. M. Zurek, Phys. Rev. D **85**, 023519 (2012).
[31] M. I. Gresham and K. M. Zurek, Phys. Rev. D **99**, 083008 (2019).
[32] O. Ivanytskyi, V. Sagun, and I. Lopes, Phys. Rev. D **102**, 063028 (2020).
[33] L. B. Okun', Phys. Usp. **50**, 380 (2007).
[34] F. Sandin and P. Ciarcelluti, Astropart. Phys. **32**, 278 (2009).
[35] M. Hippert, J. Setford, H. Tan, D. Curtin, J. Noronha-Hostler, and N. Yunes, Phys. Rev. D **106**, 035025 (2022).
[36] L. D. Duffy and K. van Bibber, New J. Phys. **11**, 105008 (2009).
[37] A. V. Balatsky, B. Fraser, and H. S. Røising, Phys. Rev. D **105**, 023504 (2022).
[38] D. M. Jacobs, G. D. Starkman, and B. W. Lynn, Mon. Not. R. Astron. Soc. **450**, 3418 (2015).
[39] S. Ge, K. Lawson, and A. Zhitnitsky, Phys. Rev. D **99**, 116017 (2019).
[40] J. P. VanDevender, R. G. Schmitt, N. McGinley, D. G. Duggan, S. McGinty, A. P. VanDevender, P. Wilson, D. Dixon, H. Girard, and J. McRae, Universe **7**, 116 (2021).
[41] A. Zhitnitsky, Mod. Phys. Lett. A **36**, 2130017 (2021).
[42] T. Kodama and M. Yamada, Prog. Theor. Phys. **47**, 444 (1972).
[43] G. L. Comer, D. Langlois, and L. M. Lin, Phys. Rev. D **60**, 104025 (1999).
[44] C. Kouvaris and P. Tinyakov, Phys. Rev. D **82**, 063531 (2010).
[45] J. Bramante and F. Elahi, Phys. Rev. D **91**, 115001 (2015).
[46] M. Baryakhtar, J. Bramante, S. W. Li, T. Linden, and N. Raj, Phys. Rev. Lett. **119**, 131801 (2017).
[47] M. Deliyergiyev, A. Del Popolo, L. Tolos, M. Le Delliou, X. Lee, and F. Burgio, Phys. Rev. D **99**, 063015 (2019).
[48] I. Goldman, R. N. Mohapatra, S. Nussinov, D. Rosenbaum, and V. Teplitz, Phys. Lett. B **725**, 200 (2013).
[49] C. Kouvaris and N. G. Nielsen, Phys. Rev. D **92**, 063526 (2015).
[50] J. Eby, C. Kouvaris, N. G. Nielsen, and L. C. R. Wijewardhana, J. High Energy Phys. 02 (2016) 028.
[51] A. Maselli, P. Pnigouras, N. G. Nielsen, C. Kouvaris, and K. D. Kokkotas, Phys. Rev. D **96**, 023005 (2017).
[52] J. Ellis, G. Hütsi, K. Kannike, L. Marzola, M. Raidal, and V. Vaskonen, Phys. Rev. D **97**, 123007 (2018).
[53] A. E. Nelson, S. Reddy, and D. Zhou, J. Cosmol. Astropart. Phys. 07 (2019) 012.
[54] F. Di Giovanni, S. Fakhry, N. Sanchis-Gual, J. C. Degollado, and J. A. Font, Phys. Rev. D **102**, 084063 (2020).
[55] M. Colpi, S. L. Shapiro, and I. Wasserman, Phys. Rev. Lett. **57**, 2485 (1986).
[56] F. E. Schunck and E. W. Mielke, Classical Quantum Gravity **20**, R301 (2003).
[57] S. L. Liebling and C. Palenzuela, Living Rev. Relativity **15**, 6 (2012).
[58] S.-C. Leung, M.-C. Chu, and L.-M. Lin, Phys. Rev. D **84**, 107301 (2011).
[59] A. Li, F. Huang, and R.-X. Xu, Astropart. Phys. **37**, 70 (2012).
[60] L. Tolos and J. Schaffner-Bielich, Phys. Rev. D **92**, 123002 (2015).
[61] A. Del Popolo, M. Deliyergiyev, and M. Le Delliou, Phys. Dark Universe **30**, 100622 (2020).
[62] H. C. Das, A. Kumar, B. Kumar, S. Biswal, and S. Patra, J. Cosmol. Astropart. Phys. 01 (**2021**) 007.
[63] S.-H. Yang, C.-M. Pi, and X.-P. Zheng, Phys. Rev. D **104**, 083016 (2021).
[64] B. Kain, Phys. Rev. D **103**, 043009 (2021).

[65] I. Lopes, J. Casanellas, and D. Eugénio, Phys. Rev. D **83**, 063521 (2011).
[66] A. Del Popolo, M. Le Delliou, and M. Deliyergiyev, Universe **6**, 222 (2020).
[67] N. F. Bell, G. Busoni, T. F. Motta, S. Robles, A. W. Thomas, and M. Virgato, Phys. Rev. Lett. **127**, 111803 (2021).
[68] T. N. Maity and F. S. Queiroz, Phys. Rev. D **104**, 083019 (2021).
[69] F. Anzuini, N. F. Bell, G. Busoni, T. F. Motta, S. Robles, A. W. Thomas, and M. Virgato, J. Cosmol. Astropart. Phys. 11 (2021) 056.
[70] D. Bose, T. N. Maity, and T. S. Ray, J. Cosmol. Astropart. Phys. 05 (2022) 001.
[71] D. Gonzalez and A. Reisenegger, Astron. Astrophys. **522**, A16 (2010).
[72] B. Bertoni, A. E. Nelson, and S. Reddy, Phys. Rev. D **88**, 123505 (2013).
[73] R. Garani, A. Gupta, and N. Raj, Phys. Rev. D **103**, 043019 (2021).
[74] J. Coffey, D. McKeen, D. E. Morrissey, and N. Raj, Phys. Rev. D **106**, 115019 (2022).
[75] M. Fujiwara, K. Hamaguchi, N. Nagata, and J. Zheng, Phys. Rev. D **106**, 055031 (2022).
[76] A. de Lavallaz and M. Fairbairn, Phys. Rev. D **81**, 123521 (2010).
[77] J. Bramante, K. Fukushima, and J. Kumar, Phys. Rev. D **87**, 055012 (2013).
[78] J. Bramante and T. Linden, Phys. Rev. Lett. **113**, 191301 (2014).
[79] D. Liang and L. Shao, J. Cosmol. Astropart. Phys. 08 (2023) 016.
[80] K. Yagi and N. Yunes, Phys. Rev. D **88**, 023009 (2013).
[81] K. Yagi and N. Yunes, Science **341**, 365 (2013).
[82] K. Yagi and N. Yunes, Phys. Rep. **681**, 1 (2017).
[83] D. A. Godzieba, R. Gamba, D. Radice, and S. Bernuzzi, Phys. Rev. D **103**, 063036 (2021).
[84] P. Routaray, A. Quddus, K. Chakravarti, and B. Kumar, Mon. Not. R. Astron. Soc. **525**, 5492 (2023).
[85] P. Thakur, T. Malik, A. Das, T. K. Jha, and C. Providência, Phys. Rev. D **109**, 043030 (2024).
[86] K. Zhang, T. Hirayama, L.-W. Luo, and F.-L. Lin, Phys. Lett. B **801**, 135176 (2020).
[87] K. Zhang, G.-Z. Huang, J.-S. Tsao, and F.-L. Lin, Eur. Phys. J. C **82**, 366 (2022).
[88] B. P. Abbott *et al.* (LIGO Scientific and Virgo Collaborations), Phys. Rev. Lett. **119**, 161101 (2017).
[89] B. P. Abbott *et al.*, Astrophys. J. Lett. **892**, L3 (2020).
[90] R. Abbott *et al.*, Astrophys. J. Lett. **896**, L44 (2020).
[91] A. Quddus, G. Panotopoulos, B. Kumar, S. Ahmad, and S. K Patra, J. Phys. G **47**, 095202 (2020).
[92] W. Husain and A. W. Thomas, J. Cosmol. Astropart. Phys. 10 (2021) 086.
[93] K.-L. Leung, M.-C. Chu, and L.-M. Lin, Phys. Rev. D **105**, 123010 (2022).
[94] D. Rafiei Karkevandi, S. Shakeri, V. Sagun, and O. Ivanytskyi, Phys. Rev. D **105**, 023001 (2022).
[95] Y. Dengler, J. Schaffner-Bielich, and L. Tolos, Phys. Rev. D **105**, 043013 (2022).
[96] M. Collier, D. Croon, and R. K. Leane, Phys. Rev. D **106**, 123027 (2022).
[97] M. Dutra, C. H. Lenzi, and O. Lourenço, Mon. Not. R. Astron. Soc. **517**, 4265 (2022).
[98] R. F. Diedrichs, N. Becker, C. Jockel, J.-E. Christian, L. Sagunski, and J. Schaffner-Bielich, Phys. Rev. D **108**, 064009 (2023).
[99] D. Rafiei Karkevandi, S. Shakeri, V. Sagun, and O. Ivanytskyi, in *The Sixteenth Marcel Grossmann Meeting* (World Scientific, Singapore, 2023).
[100] H. C. Das, A. Kumar, S. K. Biswal, and S. K. Patra, Phys. Rev. D **104**, 123006 (2021).
[101] M. Emma, F. Schianchi, F. Pannarale, V. Sagun, and T. Dietrich, Particles **5**, 273 (2022).
[102] A. Bauswein, G. Guo, J. Lien-Hua, Y.-H. Lin, and M.-R. Wu, Phys. Rev. D **107**, 083002 (2023).
[103] K. Zhang, L.-W. Luo, J.-S. Tsao, C.-S. Chen, and F.-L. Lin, Results Phys. **53**, 106967 (2023).
[104] Z. Miao, Y. Zhu, A. Li, and F. Huang, Astrophys. J. **936**, 69 (2022).
[105] S. Shakeri and D. R. Karkevandi, Phys. Rev. D **109**, 043029 (2024).
[106] H.-M. Liu, J.-B. Wei, Z.-H. Li, G. F. Burgio, and H.-J. Schulze, Phys. Dark Universe **42**, 101338 (2023).
[107] Z. H. Li, U. Lombardo, H.-J. Schulze, and W. Zuo, Phys. Rev. C **77**, 034316 (2008).
[108] Z. H. Li and H.-J. Schulze, Phys. Rev. C **78**, 028801 (2008).
[109] H.-M. Liu, J. Zhang, Z.-H. Li, J.-B. Wei, G. F. Burgio, and H.-J. Schulze, Phys. Rev. C **106**, 025801 (2022).
[110] M. Baldo, ed., *Nuclear Methods and The Nuclear Equation of State* (World Scientific, Singapore, 1999).
[111] M. Baldo and G. F. Burgio, Rep. Prog. Phys. **75**, 026301 (2012).
[112] J.-B. Wei, J.-J. Lu, G. F. Burgio, Z.-H. Li, and H.-J. Schulze, Eur. Phys. J. A **56**, 63 (2020).
[113] G. F. Burgio, H.-J. Schulze, I. Vidaña, and J.-B. Wei, Prog. Part. Nucl. Phys. **120**, 103879 (2021).
[114] G. F. Burgio, H.-J. Schulze, I. Vidaña, and J.-B. Wei, Symmetry **13**, 400 (2021).
[115] J. Antoniadis *et al.*, Science **340**, 1233232 (2013).
[116] Z. Arzoumanian *et al.*, Astrophys. J. Suppl. Ser. **235**, 37 (2018).
[117] H. T. C. *et al.*, Nat. Astron. **4**, 72 (2020).
[118] T. E. Riley *et al.*, Astrophys. J. Lett. **918**, L27 (2021).
[119] M. C. Miller *et al.*, Astrophys. J. Lett. **918**, L28 (2021).
[120] P. T. H. Pang, I. Tews, M. W. Coughlin, M. Bulla, C. Van Den Broeck, and T. Dietrich, Astrophys. J. **922**, 14 (2021).
[121] G. Raaijmakers, S. K. Greif, K. Hebeler, T. Hinderer, S. Nissanke, A. Schwenk, T. E. Riley, A. L. Watts, J. M. Lattimer, and W. C. G. Ho, Astrophys. J. Lett. **918**, L29 (2021).
[122] B. P. Abbott *et al.*, Phys. Rev. Lett. **121**, 161101 (2018).
[123] G. F. Burgio, A. Drago, G. Pagliara, H.-J. Schulze, and J.-B. Wei, Astrophys. J. **860**, 139 (2018).
[124] J.-B. Wei, A. Figura, G. F. Burgio, H. Chen, and H.-J. Schulze, J. Phys. G **46**, 034001 (2019).
[125] G. Narain, J. Schaffner-Bielich, and I. N. Mishustin, Phys. Rev. D **74**, 063003 (2006).

[126] S. Tulin, H.-B. Yu, and K. M. Zurek, Phys. Rev. D **87**, 115007 (2013).
[127] M. Cassing, A. Brisebois, M. Azeem, and J. Schaffner-Bielich, Astrophys. J. **944**, 130 (2023).
[128] M. Markevitch, A. H. Gonzalez, D. Clowe, A. Vikhlinin, W. Forman, C. Jones, S. Murray, and W. Tucker, Astrophys. J. **606**, 819 (2004).
[129] M. Kaplinghat, S. Tulin, and H.-B. Yu, Phys. Rev. Lett. **116**, 041302 (2016).
[130] L. Sagunski, S. Gad-Nasr, B. Colquhoun, A. Robertson, and S. Tulin, J. Cosmol. Astropart. Phys. 01 (2021) 024.
[131] A. Loeb, Astrophys. J. Lett. **929**, L24 (2022).
[132] A. B. Henriques, A. R. Liddle, and R. G. Moorhouse, Phys. Lett. B **251**, 511 (1990).
[133] S. C. Leung, M. C. Chu, and L. M. Lin, Phys. Rev. D **85**, 103528 (2012).
[134] S. Valdez-Alvarado, C. Palenzuela, D. Alic, and L. A. Ureña-López, Phys. Rev. D **87**, 084040 (2013).
[135] B. Kain, Phys. Rev. D **102**, 023001 (2020).
[136] T. Gleason, B. Brown, and B. Kain, Phys. Rev. D **105**, 023010 (2022).
[137] J. B. Hartle, Astrophys. J. **150**, 1005 (1967).
[138] T. Binnington and E. Poisson, Phys. Rev. D **80**, 084018 (2009).
[139] T. Hinderer, B. D. Lackey, R. N. Lang, and J. S. Read, Phys. Rev. D **81**, 123016 (2010).
[140] T. Damour and A. Nagar, Phys. Rev. D **81**, 084016 (2010).
[141] S. Postnikov, M. Prakash, and J. M. Lattimer, Phys. Rev. D **82**, 024016 (2010).